

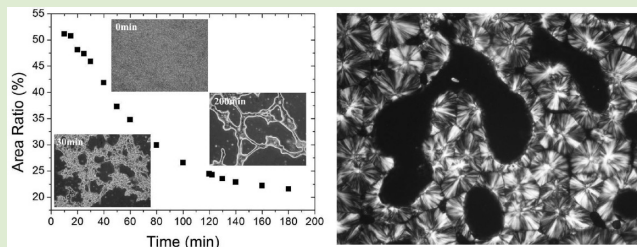
# Viscoelastic Phase Separation and Interface Assisted Crystallization in a Highly Immiscible iPP/PMMA Blend

Weichao Shi, Fenghua Chen, Yan Zhang, and Charles C. Han\*

Beijing National Laboratory for Molecular Sciences, Joint Laboratory of Polymer Science and Materials, Institute of Chemistry, Chinese Academy of Sciences, Beijing 100190, China

## Supporting Information

**ABSTRACT:** Polymer blends with dynamic asymmetry have attracted much interest recently. In this study, we report a more typical case where the dynamically asymmetric system is highly immiscible. We find that there is a transient network growth and phase inversion for the slow minor component. The network structure shows a hierarchical growth behavior, which is the result of competition between a slow relaxation-controlled concentration growth on local scale and a fast hydrodynamic growth on large scale. When phase separation couples with a subsequent crystallization, the interfacial boundary may assist lateral crystallization and irregular spherulites would grow epitaxially around the amorphous component-rich domains. The interface may play the role of substrates for heterogeneous nucleation. These phenomena may help us with morphological control in material processing.



To meet multifunctional demand (optics, conductivity, mechanics, and so on) in industrial applications, morphological control is important in polymer mixtures.<sup>1–3</sup> As most polymer pairs are thermodynamically immiscible, the conventional study finds that the minority phase should always disperse in the matrix of the majority phase.<sup>4–7</sup> This leads to less morphological variations and thus less adaptable functional properties. Recently, it has been reported that more variations of morphology can be obtained under the effect of dynamic asymmetry, which comes from the unequal mobility between component molecules.<sup>8–11</sup> A viscoelastic model has been constructed and verified when a mixture is quenched from the miscible state to an unstable state.<sup>11</sup> However, an even more typical case has not been tested: how phase separation proceeds for a highly immiscible polymer blend under the effect of dynamic asymmetry.

In addition to phase separation, crystallization is another intriguing phase transition that is usually encountered in polymer blends.<sup>1,12–16</sup> The single process of crystallization has been intensively studied in the miscible condition. But when crystallization couples with phase separation, the case becomes much more complicated.<sup>17–19</sup> One common conclusion up to now is that crystal nucleation becomes less active as phase separation proceeds.<sup>19–21</sup> It has been long predicted and expected that this phenomenon is closely related to the interfacial boundary between different phases.<sup>19,22,23</sup> Although there has been much effort on this topic, some direct macroscopic evidence is still needed. We checked the previous studies and found that conventional studies on the coupled crystallization and phase separation were usually carried out in systems with dynamic symmetry.<sup>19,24,25</sup> There are shortcomings in morphology control: first, the phase transition dynamics

cannot be easily controlled; second, there usually lacks clear interfacial boundaries; and also, phase-separated domains can be easily destroyed by crystal growth. But we believe such shortcomings can be delicately avoided in a highly immiscible blend under large dynamic asymmetry.<sup>17,18</sup>

To investigate the above two topics, we employed amorphous poly(methyl methacrylate) (PMMA) and crystalline isotactic polypropylene (iPP) for investigation. PMMA and iPP are highly immiscible in a thermodynamic sense in a large temperature and concentration range. The molecular weights of PMMA (Aladdin Reagent Inc.) and iPP (Yanshan Petrochemical Corp.) that we used in this study are  $M_w = 100$  kg/mol and  $M_w = 340$  kg/mol, respectively. The large dynamic asymmetry arises from an approximate 100 °C difference in the glass transition temperatures between the slow PMMA and the fast iPP. The two components were blended in xylene at 130 °C for 6 h, with a total weight fraction of 5%. The hot solution was quickly poured in cold methanol for coprecipitation. The sediment was dried in a vacuum oven until constant weight. For sample preparation, the solution-blended iPP/PMMA was hot-pressed at 170 °C and sandwiched in two glass plates. The sample was further trapped by silicon oil to prevent oxidation and then quickly transferred to a hot-stage for annealing. The weight ratio of PMMA is kept at 0.2 in this study.

**Hierarchical network growth and phase inversion:** Because of the large dynamic asymmetry, iPP and PMMA molecules show different responses to the thermodynamic driving force. The

Received: June 18, 2012

Accepted: August 2, 2012

Published: August 13, 2012

mobility of iPP is high at high temperatures, and the iPP-rich phase shows fluid-like behavior. However, the PMMA-rich phase is under viscoelastic effect due to much slower dynamics of PMMA molecules. The mobility contrast of each phase is enhanced as phase separation proceeds.

When the sample is annealed, the bright PMMA-rich phase covers the full screen at the beginning, in spite of the fact that PMMA is the minor component. The dark iPP-rich phase subsequently appears in the matrix, accompanied by the volume shrinking of the interconnected PMMA-rich phase. We notice that a large network starts to appear that contains many small networks on smaller scales. The rate of volume shrinking is fast in the initial stage (before 200 min), and a large network-like structure emerges when the rate is slowing down. The network-like structure stays for a long time, with thin strips bridging large PMMA-rich domains. Finally, the interconnected PMMA-rich domains break up and disperse in the matrix of iPP-rich phase (1200 min, shown in Figure 1). This is the phase inversion from a minority matrix to a usual majority matrix, which is a typical feature of the dynamically asymmetric phase separation.

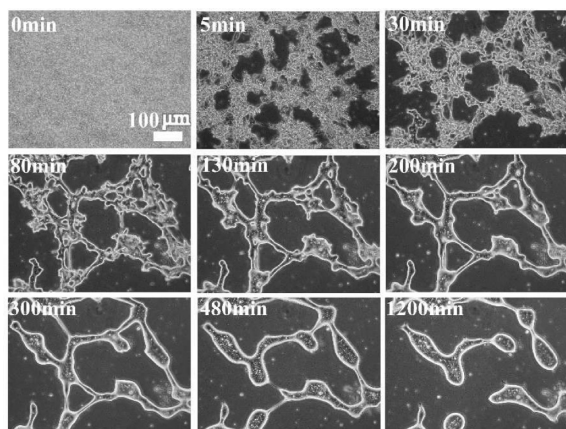


**Figure 1.** Morphological evolution of iPP/PMMA (PMMA weight fraction 0.2) blend annealed at 180 °C. The bright phase is PMMA-rich phase. The pictures were taken under phase contrast optical microscopy.

Here we should point out that there is a hierarchical growth of the network structures on different scales (as shown in Figure 1), which is different from a normal phase separation, as quenched from a miscible state.<sup>8,10</sup> Although the immiscible iPP/PMMA is homogenized by solution blending and subsequent sedimentation, the local concentration grows quickly and forms a network structure as the sample is annealed (0 min). But this local network growth is much slower than the growth on a larger scale. The original network, which covers the full screen, breaks up randomly with an emergence of a network structure on a larger scale. The quick emergence of the large network is assisted by the hydrodynamic interaction associated with fast diffusion of iPP. As the local network merges and coarsens in a small length scale, the volume of the large network shrinks and keeps the shape transiently (from 200 to 1200 min). We notice that the growth of the small network leaves many concentrated small PMMA spheres in the large PMMA-rich domains as well as in the iPP-rich phase (the small bright dots in Figure 1, see also in Figure 4a). This is the unique feature of this hierarchical growth of the network

structure. The late stage coarsening of phase separation usually shows self-similar growth in dynamically symmetric blends.<sup>7</sup> However, the self-similar growth breaks down in dynamically asymmetric blends because of the competition between molecular relaxation and interfacial tension.

Based on the viscoelastic model proposed by H. Tanaka,<sup>11</sup> the phase inversion process should contain two kinds of relaxation, ascribed to bulk and shear stress, respectively.

The slow PMMA molecules may not respond immediately to the thermodynamic instability, thus, there is a depression of the driving force mainly in the direction of concentration gradient. This is the origin of bulk stress. The effective osmotic pressure is thus expressed as  $\pi_{\text{eff}} = (\phi((\partial F)/(\partial \phi)) - F) - \int_{-\infty}^t dt' G_b(t - t') \nabla \cdot v(t')$ , where the first term denotes the thermodynamic instability and the second term is the bulk stress sustained by the slow component. Accordingly, the minority PMMA-rich phase cannot reach the equilibrium state immediately even when the system is highly thermodynamically unstable (Figure 2). The volume shrinking is the result of competition between

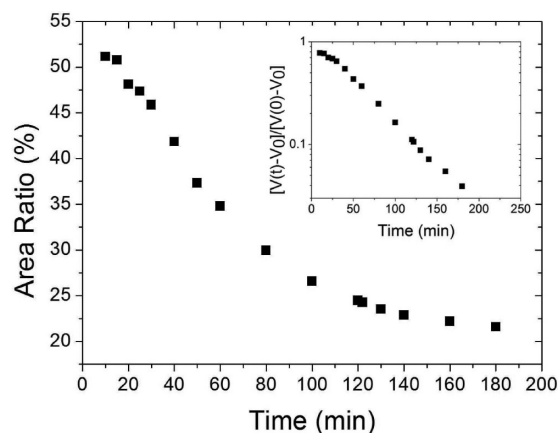


**Figure 2.** Temporal behavior of the covered area for the PMMA-rich phase when the sample was annealed at 180 °C. A fitting was drawn as the inset via an exponential relation  $(V(t) - V_0)/(V(0) - V_0) = \exp(-t/\tau_{\text{vs}})$ .

slow dynamic relaxation and the large thermodynamic instability. The slowing down of volume shrinking indicates that the system approaches to a state close to the equilibrium concentration.

The slow relaxation of PMMA molecules is also sustained with the long/thin strip structure for a long time. This is contributed mainly by shear stress. Here the shear stress frustrates the role of surface tension. In the dynamically symmetric case, the long/thin strips cannot survive long because of interface instability. In this study, we should note that the coarsening is returned and dominated by surface tension when shear stress is fully relaxed after a long time.

We plotted the covering area ratio of the PMMA-rich phase versus time. The volume decays initially with a fast rate and finally approaches a constant value (around 20%). We may also find a characteristic time  $\tau_{\text{vs}}$  to denote the volume shrinking rate via the relation  $(V(t) - V_0)/(V(0) - V_0) = \exp(-t/\tau_{\text{vs}})$ , where  $V(0)$  and  $V_0$  denote initial and final areas of the PMMA-rich phase. The values of  $\tau_{\text{vs}}$  at 200, 190, 180, and 170 °C are 3.6, 6.5, 53.7, and 155.0 min, respectively. The strong dependence of  $\tau_{\text{vs}}$  is the result of strong dependence of PMMA relaxation with respect to bulk stress as the temperature approaches the glass transition of neat PMMA. The

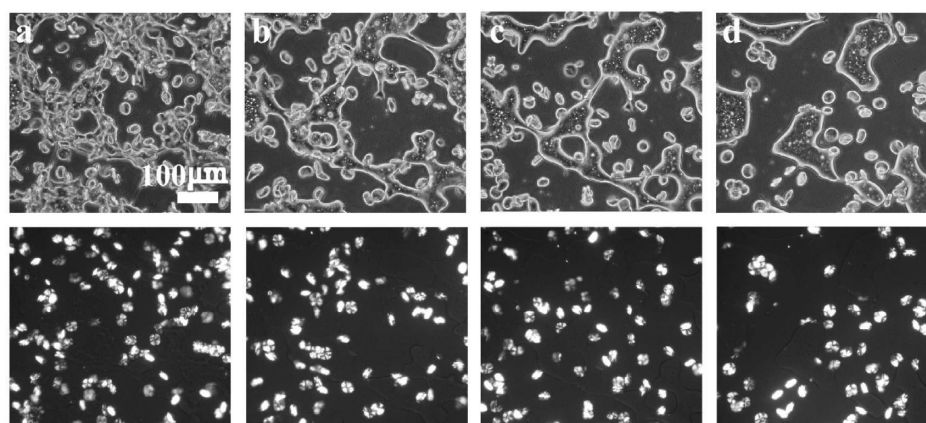


**Figure 3.** Effect of phase separation on subsequent nucleation. The sample was first annealed for phase separation at 180 °C for (a) 30, (b) 100, (c) 300, and (d) 1500 min, respectively, and then quenched to 140 °C for crystallization for 10 min. The pictures in the upper row were taken under phase contrast optical microscopy and the bottom row under polarized optical microscopy.

thermodynamic immiscibility gives the origin of the small network and the hierarchical growth arises from the fast hydrodynamic interaction of the iPP-rich phase and the slow relaxation of the bulk stress. The even slower relaxation of the shear stress is responsible for keeping the shape of the large network structure transiently. When the shear stress relaxes, the interface energy breaks up the large network structure.

The roles of bulk stress and shear stress are more important when the temperature is lowered close to the glass transition temperature of PMMA. The blend approaches a dynamically symmetric case when both components behave fluid-like at high temperatures. So the phase separation dynamics can be largely mediated via annealing temperature.

**Interface-assisted crystallization:** To investigate the effect of phase separation on crystallization, we applied a double-quench method. The sample was first annealed at 180 °C for different times and then quenched to lower temperatures for crystallization. Because the phase separation dynamics is much slower at lower temperatures, we do not have to consider the effect of a secondary phase separation on subsequent crystallization. This is an additional advantage compared with a dynamically symmetric blend.

First, we investigate crystal nucleation under the effect of phase separation. The longer the phase separation proceeds at a higher temperature, the slower the nucleation rate is at a lower temperature. This tendency is obviously revealed in Figure 3. The nucleation density in Figure 3a is about two times that in Figure 3d. Moreover, we can check the location of nucleation clearly. We note that as phase separation proceeds longer at the higher temperature, the nucleation is more likely to take place at iPP-rich phase. However, when there is the hierarchical network structure initially, the nucleation is more likely to grow at the edge of the interface. The role of the interface can also be detected by differential scanning calorimeter (DSC) when the sample was cooled with a rate of 10 °C/min. As the phase separation proceeds longer at a higher temperature, the optimal crystallization temperature shifts to lower values (see Supporting Information, Figure 1).

There is an epitaxial growth layer around the PMMA-rich domains. Here we show one more picture of the final morphology when the sample was annealed for crystallization (at 130 °C) after phase separation (at 180 °C for 1200 min). As shown in Figure 4, irregular spherulites grew around the large PMMA-rich phase (see Supporting Information, Figure 2).

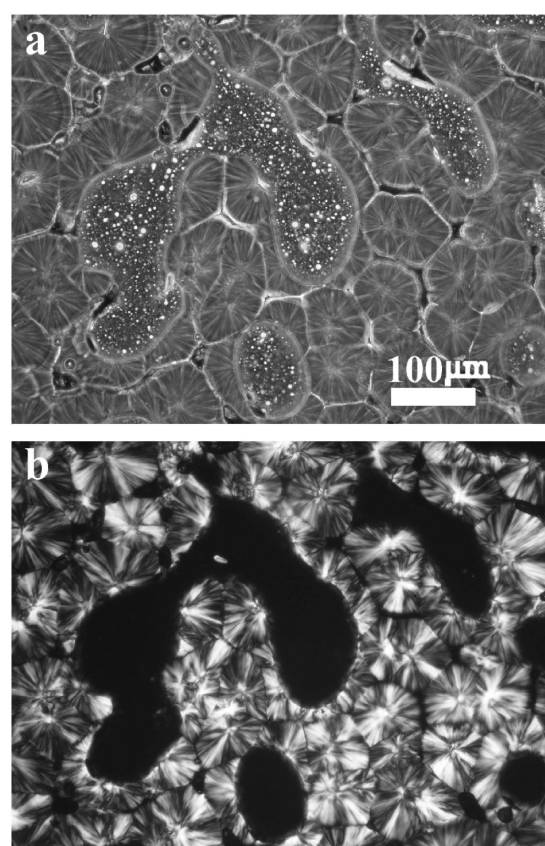


**Figure 4.** Final morphology of iPP/PMMA blend when the sample was first phase separated at 180 °C for 1200 min and then crystallized at 130 °C for 30 min: (a) taken under phase contrast optical microscopy and (b) under polarized optical microscopy.

This provides direct macroscopic evidence for interface-assisted crystallization.

Although it was predicted and expected that crystallization is assisted at the interface,<sup>19,22,23</sup> there has not been convincing evidence from a macroscopic scale. In previous studies, crystal growth at the interface was usually selectively captured in a small region (usually under electron microscopy or atomic force microscopy).<sup>19,20</sup> However, the smeared interface, hydrodynamic distortion of the amorphous-rich phase and the irregular crystal growth made the result questionable. In

contrast, in this highly immiscible dynamically asymmetric blend, all the shortcomings can be delicately avoided. Because of highly immiscibility, the equilibrium composition of each phase is not much different from the bulk condition. The interface becomes sharp and phase separated domains grow on a large scale from a very early stage, while the dynamics can be easily mediated via annealing temperature. As the experimental temperature is not much above the glass transition of PMMA, the concentrated PMMA-rich phase cannot be easily distorted by hydrodynamic interaction.

The physical origin of interface-assisted crystallization is still under debate. One interpretation focuses on the dynamic origin of concentration fluctuation, which proposes that interdiffusion at the interface may lead to conformational ordering and thus lower the energy barrier for nucleation. This idea has been supported by some recent work.<sup>17–21</sup> Another one attributes the static to the heterogeneous nucleation at the interface.<sup>22</sup> In our opinion, both of these factors contribute to the nucleation in dynamically symmetric blends (see Supporting Information, Figure 3). However, for this iPP/PMMA blend, the phase-separation dynamics is severely suppressed at lower temperatures so that the concentration fluctuation and the interdiffusion at the interface are suppressed and can be neglected in this case, so we can observe the interface-assisted crystallization by the static heterogeneous nucleation at the interface only.

Controlling the morphology is crucially important for controlling the mechanical properties of materials. As the minor phase can invert from the transient network to dispersed domains, the mechanical properties can have more possibilities varied between the properties of neat iPP and neat PMMA. The interfacial property is the other parameter that may be controlled. In the usual immiscible blend, the sharp boundary indicates weak adhesion and cannot sustain much applied strength. To enhance the relationship between two immiscible phases, compatibilizer (like block copolymers, chemical modification, or additives) is usually the choice.<sup>26,27</sup> In this blend, however, the crystallization at the interface can play the role of varying the interfacial properties. We hope the current work may stimulate more attention on dynamically asymmetric blends for fundamental research as well as material processing.

## ■ ASSOCIATED CONTENT

### 📄 Supporting Information

Supporting figures. This material is available free of charge via the Internet at <http://pubs.acs.org>.

## ■ AUTHOR INFORMATION

### Corresponding Author

\*E-mail: [c.c.han@iccas.ac.cn](mailto:c.c.han@iccas.ac.cn). Phone: +86 10 82618089. Fax: +86 10 62521519.

### Notes

The authors declare no competing financial interest.

## ■ ACKNOWLEDGMENTS

This work is supported by the National Basic Research Program of China (973 Program, 2012CB821503) and National Natural Science Foundation of China (No. 50930003).

## ■ REFERENCES

- (1) Paul, D. R.; Newman, S. *Polymer Blends*; Academic Press: New York, 1978.
- (2) Araki, T.; Qui, T.-C.; Shibayama, M. *Structure and Properties of Multiphase Polymeric Materials*; M. Dekker: New York, 1998.
- (3) Zhang, Y.; Shi, W.; Chen, F.; Han, C. C. *Macromolecules* **2011**, *44*, 7465–7472.
- (4) de Gennes, P. G. *J. Chem. Phys.* **1980**, *72*, 4756–4763.
- (5) Pincus, P. *J. Chem. Phys.* **1981**, *75*, 1996–2000.
- (6) Binder, K. *J. Chem. Phys.* **1983**, *79*, 6387–6409.
- (7) Hashimoto, T. *Phase Transitions* **1988**, *12*, 47–119.
- (8) Tanaka, H. *Macromolecules* **1992**, *25*, 6377–6380.
- (9) Tanaka, H. *Phys. Rev. Lett.* **1998**, *81*, 389–392.
- (10) Tanaka, H. *Phys. Rev. Lett.* **1996**, *76*, 787–790.
- (11) Tanaka, H. *J. Phys.: Condens. Matter* **2000**, *12*, R207–R264.
- (12) Cheng, S. Z. D. *Phase Transitions in Polymers: The Role of Metastable States*; Elsevier: Amsterdam, Boston, 2008.
- (13) Lorenzo, M. L. D. *Prog. Polym. Sci.* **2003**, *28*, 663–689.
- (14) Keller, A.; Cheng, S. D. Z. *Polymer* **1998**, *39*, 4461–4487.
- (15) Hoffman, J. D.; Miller, R. *Polymer* **1997**, *38*, 3151–3212.
- (16) Strobl, G. *Prog. Polym. Sci.* **2006**, *31*, 398–442.
- (17) Shi, W.; Han, C. C. *Macromolecules* **2012**, *45*, 336–346.
- (18) Shi, W.; Yang, J.; Zhang, Y.; Luo, J.; Liang, Y.; Han, C. C. *Macromolecules* **2012**, *45*, 941–950.
- (19) Zhang, X.; Wang, Z.; Dong, X.; Wang, D.; Han, C. C. *J. Chem. Phys.* **2006**, *125*, 024907(1–10).
- (20) Hong, S.; Zhang, X.; Zhang, R.; Wang, L.; Zhao, J.; Han, C. C. *Macromolecules* **2008**, *41*, 2311–2314.
- (21) Arai, F.; Takeshita, H.; Dobashi, M.; Takenaka, K.; Miya, M.; Shiomi, T. *Polymer* **2012**, *53*, 851–856.
- (22) Mitra, M. K.; Muthukumar, M. *J. Chem. Phys.* **2010**, *132*, 184908(1–6).
- (23) Ma, Y.; Zha, L.; Hu, W.; Reiter, G.; Han, C. C. *Phys. Rev. E* **2008**, *77*, 061801(1–5).
- (24) Chuang, W. T.; Jeng, U. S.; Hong, P. D.; Sheu, H. S.; Lai, Y. H.; Shih, K. S. *Polymer* **2007**, *48*, 2919–2927.
- (25) Wang, H.; Shimizu, K.; Kim, H.; Hobbie, E. K.; Wang, Z.-G.; Han, C. C. *J. Chem. Phys.* **2002**, *116*, 7311–7315.
- (26) Li, H.; Yan, S. *Macromolecules* **2011**, *44*, 417–428.
- (27) Wang, D.; Li, Y.; Xie, X. M.; Guo, B. H. *Polymer* **2011**, *52*, 191–200.